Strojniški vestnik - Journal of Mechanical Engineering 62(2016)2, 79-85
DOI:10.5545/sv-jme.2015.2840
Original Scientific Paper
Received for review: 2015-07-09
Received revised form: 2015-10-01
Accepted for publication: 2015-12-21

Manufacturing and Properties of a Magnesium Interpenetrating Phase Composite

Matej Steinacher[1,*] – Borut Žužek[2] – Darja Jenko[2] – Primož Mrvar[3] – Franc Zupanič[1]

[1] University of Maribor, Faculty of Mechanical Engineering, Slovenia
[2] Institute of Metals and Technology, Slovenia
[3] University of Ljubljana, Faculty of Natural Sciences and Engineering, Slovenia

The manufacturing and properties of the AE44 magnesium alloy reinforced with SiC–Al_2O_3–SiO_2 ceramic foam were studied. The interpenetrating phase composite was manufactured by gravity casting at different preheating temperatures of the ceramic foam. The samples were investigated using optical and electron microscopy, energy dispersive X-ray spectroscopy, X-ray diffraction, transmission electron microscopy and compression testing. The interfacial reaction products (AlSiRE and AlMgSiRE) between the metal phase and ceramics were influenced by the preheating temperatures of ceramic foam and reduced the compression strength significantly.

Keywords: AE44 magnesium alloy, ceramic foam, interpenetrating phase composite, reaction product, mechanical properties

Highlights

- *The interpenetrating phase composite was produced by gravity casting.*
- *The AE44 Mg-alloy and SiC-Al_2O_3-SiO_2 ceramic foam were used.*
- *The AE44 Mg-alloy strongly reacted with the SiC-Al_2O_3-SiO2 ceramics.*
- *The main interfacial reaction products were MgO, AlSiRE, and AlMgSiRE.*
- *The hard AlSiRE and AlMgSiRE decreased mechanical properties.*

0 INTRODUCTION

Metal-matrix composites (MMCs) show improved performances over their matrix alloys. Magnesium matrix composites can offer potential applications within the automobile and aircraft industries. Interpenetrating phase composites (IPCs) usually display superior mechanical properties when compared to conventional MMCs reinforced with particles, intermetallic phases, ceramics, and carbon fibres. A unique combination of cellular ceramic materials, with high mechanical strength and stiffness at low fractional densities, and the ductility of the metallic phase may be considered as a major advantage of metal/ceramic IPCs [1]. They can be produced using various ways [2] and [3]. The infiltration can be achieved by a spontaneous capillary-driven metal infiltration [4], gas pressure-assisted infiltration [5] and [6], or squeeze-casting into a cellular ceramic preform [1], [7] and [8]. Interface behaviour between the matrix and the reinforcement can profoundly affect the properties of the MMCs [9]. The reinforcement type, alloying elements, solidification condition, and heat-treatment of MMCs can affect the local chemical composition and the extent of the interfacial reactions of the MMCs [10].

Several IPCs with Mg-matrix have been reported [1], [7] and [8]. The AZ91, and AZ31 magnesium alloys were used for the matrix, whilst the reinforcing phase was the ceramic foam based on SiO_2, SiO_2-Al_2O_3, and SiC-SiO_2-C-Si. The mechanical properties (strength and Young's modulus) of the investigated IPCs were higher by up to 50 % when compared to the unreinforced magnesium alloy at room and elevated temperature.

During this work, we used the AE44 magnesium alloy for the matrix and ceramic foam consisting of SiC, Al_2O_3, and SiO_2 as the reinforcing phase. The IPC was produced using a simple and low-cost procedure, characterised and mechanically tested. It is to be expected that different manufacturing conditions can profoundly affect the properties of the resulting composite.

1 EXPERIMENTAL

An AE44 magnesium alloy and SiC-Al_2O_3-SiO_2 ceramic foam were used for manufacturing the IPC. The composition of the AE44 alloy was determined using ICP-AES (Table 1a). Polyurethane foam of the desired shape (Fig. 1a) was used as a preform for the manufacturing of the ceramic foam (Fig. 1b). Low viscous ceramic slurry (Table 1b) was infiltrated into a polyurethane preform. The excessive slurry was squeezed-out, and the coated preform was dried. Finally, it was heat-treated in order to remove the polyurethane skeleton and to sinter the ceramic powder. The ceramic foam is commercially accessible

*Corr. Author's Address: University of Maribor, Faculty of Mechanical Engineering, Smetanova ulica 17, 2000 Maribor, Slovenia, matej.steinacher@gmail.com

(ETI d.d.) and is used for filtration of the melt before the casting, because it is stable up to a temperature of 1700 °C.

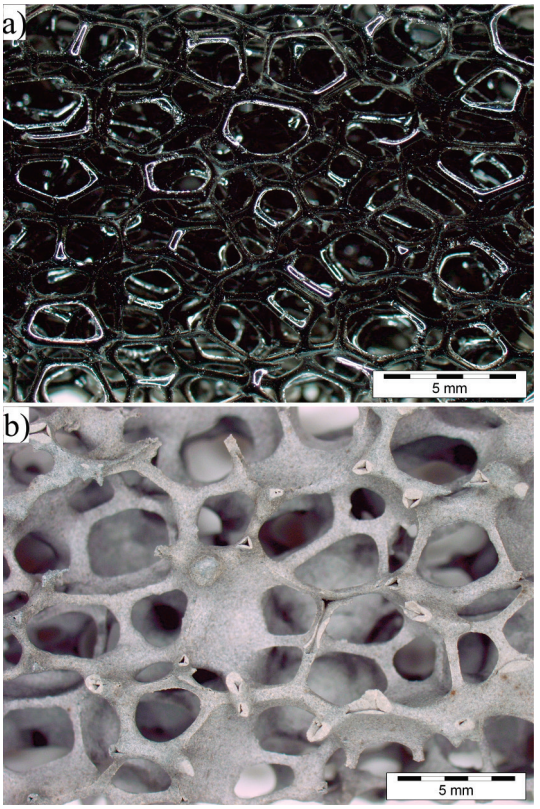

Fig. 1. *The cellular material; a) a polyurethane preform and b) a ceramic foam*

Table 1. *The chemical composition of the AE44 alloy and ceramics (wt. %)*

a) The AE44 magnesium alloy				
Al	Mn	Zn	Si	Ce
4.94	0.21	0.03	0.02	1.95
La	Nd	Pr	Mg	
1.71	0.48	0.28	Balance	
b) The ceramics				
SiC	Al_2O_3	SiO_2	Fe_2O_3	CaO
72.3	18.3	8.8	0.5	0.1

The IPC was made in several steps. A steel mould (Fig. 2) with a properly sized gating system and coated with a boron-nitride was made first. The gating system provided sufficient metal-static pressure that the melt could fill all pores of the ceramic foam. The ceramic foam had been inserted into the mould cavity before the mould was closed with the second part. Then the mould with inserted ceramic foam was preheated to a temperature of 500 °C, 600 °C, or 700 °C. During heating, the AE44 magnesium alloy was induction-melted and heated to a casting temperature of 730 °C. When the mould with inserted ceramic foam attained a suitable temperature, it was taken out of the furnace, placed on the vibration plate, and the melt was gravity cast through the inlet channel. After casting, the insulation cover was placed on the top of the mould, which acted as an insulated feeder. During the casting and solidification, the mould was vibrated so that the air from the pores of the ceramic foam and the mould cavity was removed. The metallic vibration plate transferred the heat from the bottom of the mould very well and thus enabled directional solidification. The AE44 magnesium alloy was also cast into the mould under the same conditions as ICP.

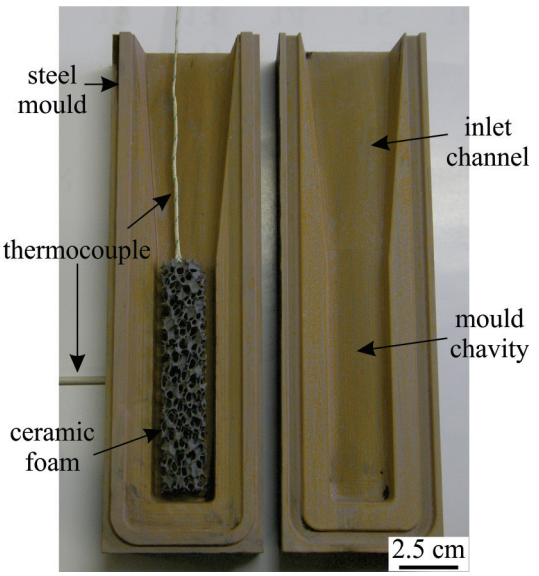

Fig. 2. *The mould with an inserted ceramic foam*

For the stress-strain measurements the samples with square cross-section (7 mm × 7 mm × 9.5 mm) were cut from the ICP and AE44 alloy. The ICP's samples contained 10.9 to 25.5 vol. % ceramics. The compression tests were carried out at room temperature (20 °C) and 200 °C by using Gleeble 1500D.

Light microscopy (LM) work was done using the Olympus BX61 with the Analysis Materials Research Lab 5.0 software, and the scanning electron microscopy (SEM) in a FEI SIRION NC. The transmission electron microscopy (TEM) was carried out on a FEI Tecnai F20. A TEM specimen was cut out at a specific site using the focussed ion beam (FIB) in a FEI Nova 200. The hardness was determined using a Wilson Instruments Tukon 2100 B (load of 10 N) and micro-hardness using an Agilent Nano Indenter G200 testing machine (a Berkovich diamond indenter,

depth limit of 500 nm, strain rate target of 0.05 cycles/s, harmonic displacement target of 2 nm, and a frequency target of 45 Hz). The composition of the ceramics was determined using an X-ray fluorescence (XRF) analyser Niton XL3t GOLDD+ (50 kVp). The X-ray diffraction (XRD) for the ceramics was carried out in a Philips 17-10 using Cu Kα radiation with a scan rate of 1.2 °/min, and for the alloy EA44 in a PANalytical B.V PW3830/40 using Cu Kα radiation with a scan rate of 0.25 °/min.

2 RESULTS AND DISCUSSION

2.1 The Magnesium Alloy

The characterisation of the commercial AE44 magnesium alloy using EDS-analysis showed that it consisted of α-Mg, $Al_{11}RE_3$, Al_2RE, and $Al_{10}RE_2Mn_7$. These phases were also identified using XRD-analysis. Each intermetallic compound contained all rare-earth elements; however, the content of Ce was the highest. Also other authors **[11]** to **[13]** found the same phases within microstructure of the AE44 alloy.

2.2 The Ceramic Foam

Fig. 1b shows the structure of the SiC-Al_2O_3-SiO_2 ceramic foam with the interconnected primary and mainly closed secondary porosity. The cellular-shape of the primary porosity had a mean-cell diameter of 4.23 mm, which was almost identical to the shapes and sizes of those pores in the polyurethane foam. The secondary porosity had a triangular void in the struts, which may reduce the strength significantly, is typical for reticulated foams. The mean-strut thickness was 0.55 mm. The XRD (Fig. 3) and EDS (Fig. 4, Table 2) results revealed that the ceramics was composed of four compounds: α-Al_2O_3, α-SiC, β-SiC, and SiO_2.

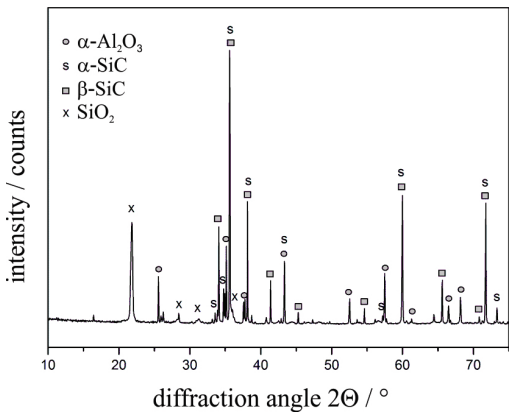

Fig. 3. *The XRD pattern of the ceramics*

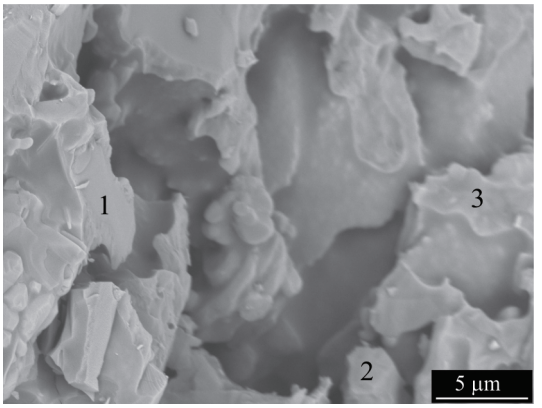

Fig. 4. *The fracture of the ceramics with sites of EDS analyses*

Table 2. The EDS analyses of the ceramics (at. %, Fig. 4)

site	C	O	Al	Si	compound
1	54.6	2.5	/	42.9	SiC
2	5.2	63.6	27.1	4.1	Al_2O_3
3	7.3	60.7	0.5	31.5	SiO_2

2.3 Interpenetrating Phase Composite

The reaction time between the melt and ceramic foam was equal to the solidification time, which was approximately 5 s, 30 s, and 60 s at the preheating temperatures of 500 °C, 600 °C, and 700 °C, respectively. During this rather short period, the melt completely filled the primary porosity, whilst the secondary porosity was filled only at preheating temperatures of 600 °C and 700 °C. The secondary porosity was probably filled by a combination of melt penetration through the strut walls and the melt infiltration through the holes in the strut walls, which represented direct links between the primary and secondary porosities. Fig. 5 shows that the melt did not just fill ceramic foam but also reacted with it. The infiltration at a preheating temperature of 500 °C resulted in the composite that suffered from partial debonding at the metal/ceramic interface and cold junctions (Fig. 5a). The widths of the cracks between the metal and ceramic skeleton were up to 50 μm. In contrast, at the preheating temperature of 600 °C (Fig. 5b) and 700 °C (Fig. 5c) obtained a crack and debonding free interfaces but with the interfacial reaction products. These were as a result several reactions between the Mg-melt, SiO_2, and Al_2O_3. The reaction products formed not only at the interfaces but also within the penetrated strut walls. The widths of the interfacial reaction products were more than 200 μm. EDS analyses (Table 3) revealed the presence

of MgO, and two intermetallic compounds with the general formulae AlSiRE and AlMgSiRE (Fig. 6), which were undetermined by XRD analysis because of their small amounts (Fig. 7).

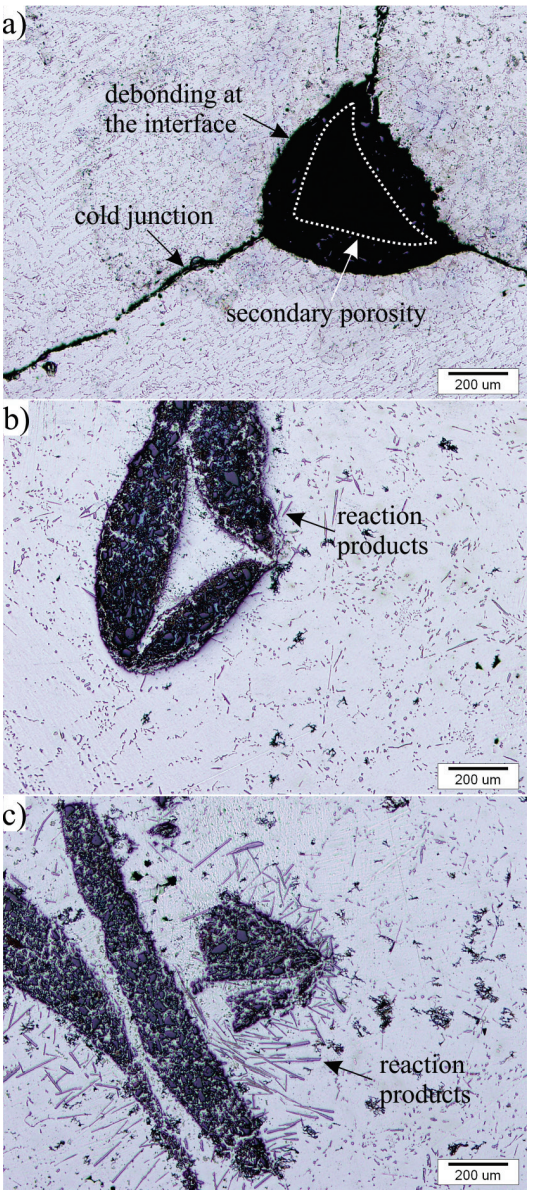

Fig. 5. *The cross-section through a strut of the IPC manufactured at the different preheating temperatures; a) 500 °C, b) 600 °C, and c) 700 °C*

Table 3. The chemical compositions of the AlSiRE and AlMgSiRE phases as determined using EDS analyses (at. %)

compound	Al	Mg	Si	Ce	La	Nd	Pr
AlSiRE	36.9	/	26.3	20.0	7.7	6.8	2.3
AlMgSiRE	14.1	24.2	33.1	16.6	6.6	3.9	1.5

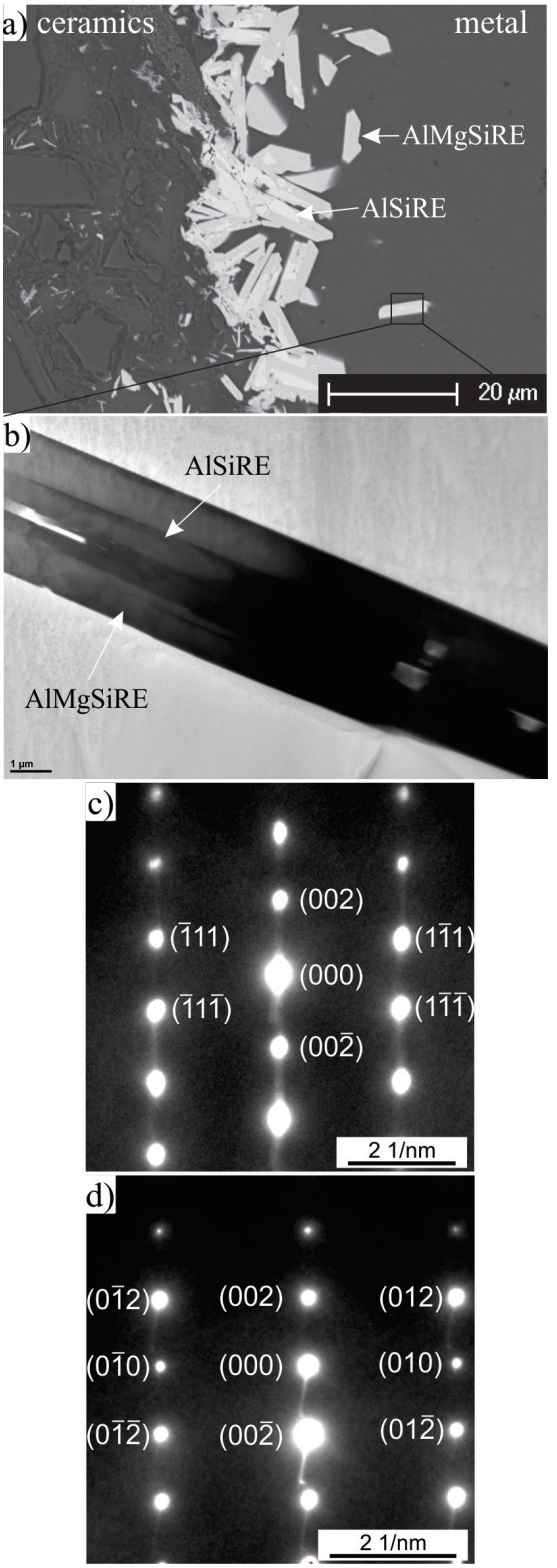

Fig. 6. *The reaction products at the metal/ceramic interface; a) SEM, b) TEM micrograph, c) SAED AlSiRE, zone axis [110], d) SAED AlMgSiRE, zone axis [100]*

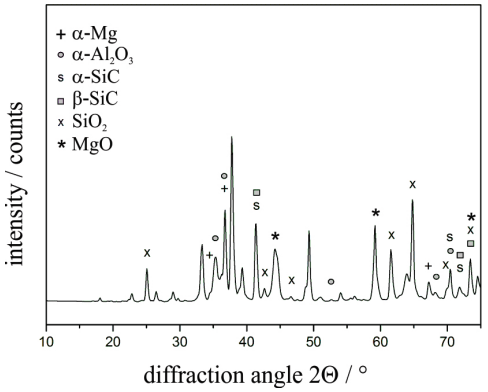

Fig. 7. *The XRD pattern of the interpenetrating phase composite*

Therefore, TEM investigations were carried out. The corresponding SAED-patterns for AlSiRE and AlMgSiRE are shown in Figs. 6c, d. Both are consistent with tetragonal structures. The AlSiRE phase always precipitated at first. It formed on the MgO film that covered the SiC and Al_2O_3. The AlSiRE particles later represented the nucleation sites for the AlMgSiRE phase. Thus, AlSiRE was usually partly or even completely surrounded by the AlMgSiRE, and the transformation from AlSiRE to AlMgSiRE took place with a reaction similar to a peritectic reaction. These compounds were presented in detail in reference [14]. The chemical reaction between Mg

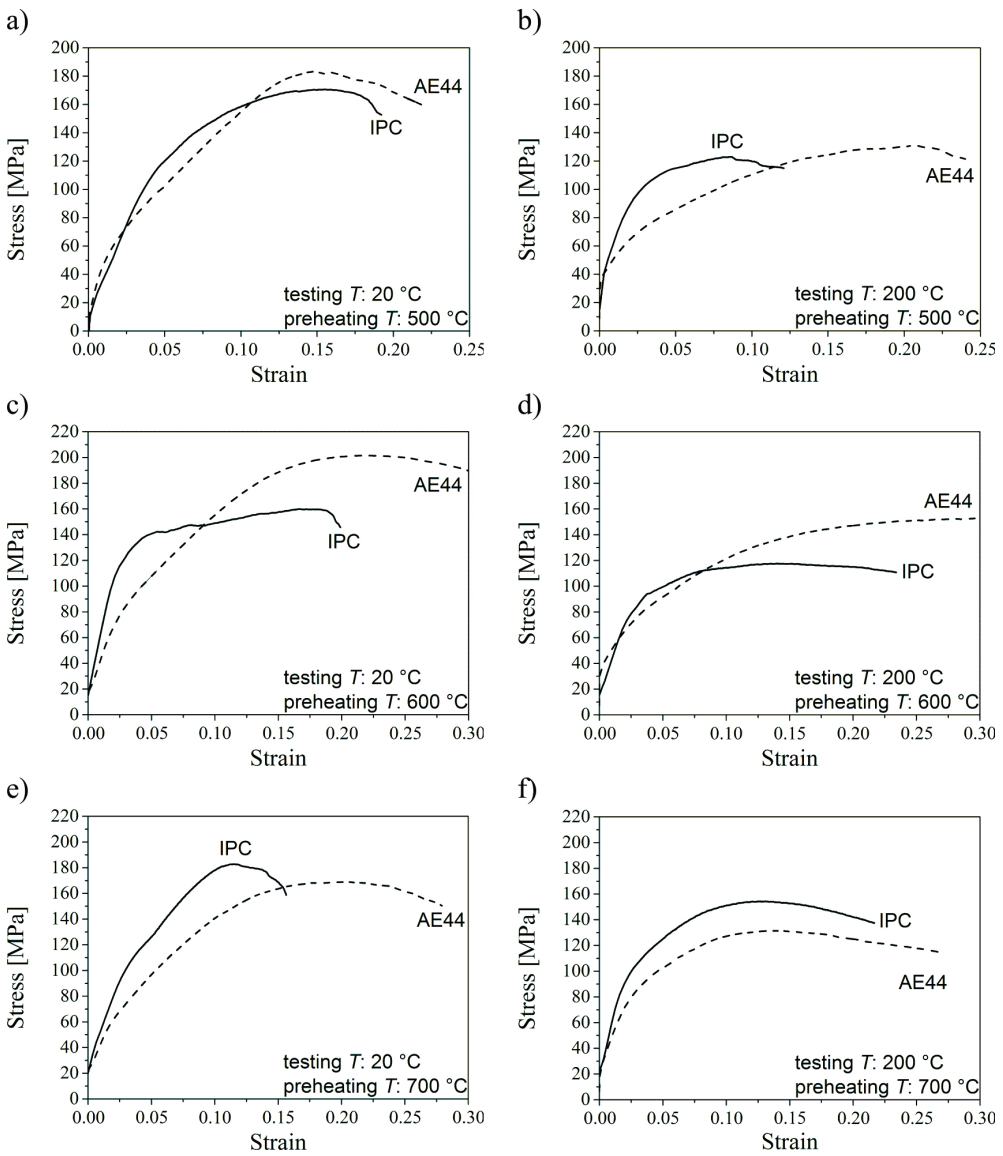

Fig. 8. *Stress-strain diagrams of the IPC and AE44 alloy manufactured at different preheating temperatures; a) and b) 500 °C, c) and d) 600 °C, e) and f) 700 °C and tested at room temperature; a), c) and e) 20 °C and b), d) and f) 200 °C*

and SiO_2, which was added as a binding agent at the manufacturing of the ceramic foam, caused the decomposition of the ceramics at the longest reaction time of 60 s (Fig. 5c).

2.4 Mechanical Properties

Fig. 8 shows the stress-strain diagrams of the IPC and AE44 alloys. At both testing temperatures (20 °C and 200 °C) the IPC showed a significant improvement of the yield strength and the Young's modulus to AE4 alloy. But the rupture modulus of the IPCs, manufactured at preheating temperatures of 500 °C and 600 °C, were lower than for the non-reinforced AE44 alloy (Figs. 8a to d), while the IPC manufactured at 700 °C had higher values (Figs. 8e and f). Gibson and Ashby, crushing of the ceramic foams is according to the micro-mechanical model of based on bending of the struts [15]. Thus, in the interpenetrating metal/ceramic phase composites, the metal phase stabilies of the ceramic struts and partially prevents strut bending. This results in a major improvement of the mechanical properties [1]. However, the IPC, made at preheating temperatures of 500 and 600 °C, showed inferior values modulus of the rupture. At 500 °C, the load transfer from the metal matrix to the reinforcing ceramic skeleton was reduced due to air gaps between the infiltrated metal and the ceramic struts. Accordingly, no pronounced reinforcing effect was observed. The firm metal/ceramic interfaces with interfacial reaction products were at 600 °C. The large interfacial reaction products, which are usually brittle and defective, decreased the compression strength of the IPC. Similarly, the tensile strength of the Ti-MMCs reinforced with SiC fibres decreased with the increase of the reaction zone but the strength was not reduced while the thickness of the interfacial reaction products was up to about 1 µm [16]. At 700 °C, the ceramic foam disintegrated into the particles and the interfacial reaction products floated into the melt. These hard particles reinforced the matrix, similarly as in the conventional metal-matrix composite reinforced with particles because the mechanical properties were higher compared to the bulk AE44.

2.5 Hardness and Micro-hardness of AlSiRE and AlMgSiRE

The measurements were carried out within the matrix and at the interface (Fig. 9a). The hardness of the matrix was 40 HV 1 and of the interface was 88 HV 1, respectively. The micro-hardness of the AlSiRE was 1336 ± 78 HV and of AlMgSiRE was 917 ± 32 HV (Fig. 9b). Thus, both phases were very hard, yet, AlSiRE was much harder than AlMgSiRE. Therefore the formations of these phases decreased in strength. On the other hand these can increase the resistance to cutting and wearing.

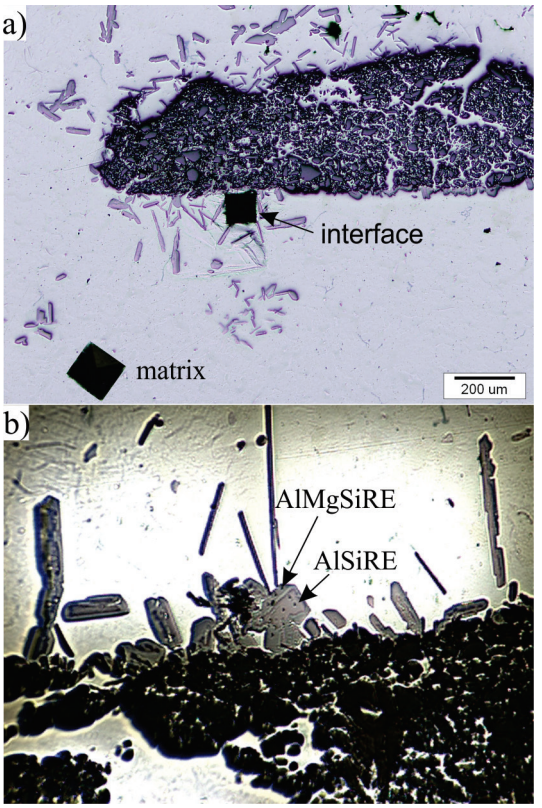

Fig. 9. *The measuring points for; a) hardness and b) micro-hardness*

3 CONCLUSIONS

According to the results of this work the following conclusions can be drawn:

- The interpenetrating phase composite can be manufactured by simple gravity casting.
- The AE44 magnesium alloy strongly reacted with the SiC-Al_2O_3-SiO_2 ceramics.
- The preheating temperature of the ceramic foam effected the bonding and interfacial reaction.
- The main reaction products were MgO and the two novel phases AlSiRE and AlMgSiRE.
- The hard AlSiRE and AlMgSiRE decreased the strength of the interpenetrating phase composite at room and elevated temperatures.
- At a preheating temperature of 700 °C the ceramic foam disintegrated into the particles, which together with reaction products floated into

the melt and reinforced the matrix, because the strength was increased.

4 ACKNOWLEDGEMENT

This work was partly financed by the Slovenian Research Agency (ARRS), projects 1000-09-310152 and L2-2269. The authors also wish to thank Mrs. Petra Juvan, ETI, for preparing the ceramics and Mr. Tomaž Martinčič, University of Ljubljana, Faculty of Natural Sciences and Engineering, for manufacturing the composite.

5 REFERENCES

[1] Zeschky, J., Lo, J., Höfner, T., Greil, P. (2005). Mg alloy infiltrated Si-O-C ceramic foams. *Materials Science and Engineering: A*, vol. 403, no. 1-2, p. 215-221, **DOI:10.1016/j.msea.2005.04.052**.

[2] Claussen, N., Urquhart, A.W. (1990). *Directed Oxidation of Molten Metals*. Pergamon Press, Oxford.

[3] Liu, W., Köster, U. (1996). Criteria for formation of interpenetrating oxide/metal-composites by immersing sacrificial oxide preforms in molten metals. *Scripta Materialia*, vol. 35, no. 1, p. 35-40, **DOI:10.1016/1359-6462(96)00084-X**.

[4] Toy, C., Scott, W.D. (1990). Ceramic-metal composite produced by melt infiltration. *Journal of the American Ceramic Society*, vol. 73, no. 1, p. 97-101, **DOI:10.1111/j.1151-2916.1990.tb05097.x**.

[5] Prielipp, H., Knechtel, M., Claussen, N., Streiffer, S.K., Müllejans, H., Rühle, M. Rödela, J. (1995). Strength and fracture toughness of aluminum/alumina composites with interpenetrating networks. *Materials Science and Engineering: A*, vol. 197, no. 1, p. 19-30, **DOI:10.1016/0921-5093(94)09771-2**.

[6] Skirl, S., Hoffman, M., Bowman, K., Wiederhorn, S., Rödel, J. (1998). Thermal expansion behavior and macrostrain of Al_2O_3/Al composites with interpenetrating networks. *Acta Materialia*, vol. 46, no. 7, p. 2493-2499, **DOI:10.1016/S1359-6454(98)80033-5**.

[7] Zeschky, J., Goetz-Neunhoeffer, F., Neubauer, J., Lo, S.H.J., Kummer, B., Scheffler, M., Greil P. (2003). Preceramic polymer derived cellular ceramics. *Composites Science and Technology*, vol. 63, no. 16, p. 2361-2370, **DOI:10.1016/S0266-3538(03)00269-0**.

[8] Zeschky, J., Lo, S.H.J., Scheffler, M., Hoeppel, H.W., Arnold, M., Greil, P. (2002). Polysiloxane-derived ceramic foam for the reinforcement of Mg alloy. *Zeitschrift für Metallkunde*, vol. 93, no. 8, p. 812-818, **DOI:10.3139/146.020812**.

[9] Kainer, K.U. (2006). Basics of Metal Matrix Composites. Kainer, K.U. (ed.). *Metal Matrix Composites: Custom-made Materials for Automotive and Aerospace Engineering*. Wiley-VCH & KGaA, Weinheim, p. 1-52, **DOI:10.1002/3527608117**.

[10] Mordike, B.L., Lukáč, P. (2001). Interfaces in magnesium-based composites. *Surface and Interface Analysis*, vol. 31, no. 7, p. 682-691, **DOI:10.1002/sia.1094**.

[11] Rzychoń, T., Kiełbus, A. (2008). Microstructure and tensile properties of sand cast and die cast AE44 magnesium alloy. *Archives of Metallurgy and Materials*, vol. 53, no. 3, p. 901-907.

[12] Zhu, S.M., Nie, J.F., Gibson, M.A., Easton, M.A., Bakke, P. (2012). Microstructure and creep behavior of high-pressure die-cast magnesium alloy AE44. *Metallurgical and Materials Transactions A*, vol. 43, p. 4137-4144, **DOI:10.1007/s11661-012-1247-9**.

[13] Rzychoń, T., Kiełbus, A., Cwajna, J., Mizera, J. (2009). Microstructural stability and creep properties of die casting Mg-4Al-4RE magnesium alloy. *Materials Characterization*, vol. 60, no. 10, p. 1107-1113, **DOI:10.1016/j.matchar.2009.05.014**.

[14] Steinacher, M., Mrvar, P., Zupanič, F. (2015). Interaction between AE44 magnesium alloy and SiC–Al_2O_3–SiO_2 ceramic foam. *Transactions of Nonferrous Metals Society of China*, vol. 25, no. 3, p. 1011-1019, **DOI:10.1016/S1003-6326(15)63692-5**.

[15] Gibson, L.J., Ashby, M.F. (1997). *Cellular Solids: Structure and Properties*, 2nd ed. Cambridge University Press, Cambridge, **DOI:10.1017/cbo9781139878326**.

[16] Onzawa, T., Suzumura, A., Kim, J.H. (1991). Influence of reaction zone thickness on tensile strength for titanium matrix composites reinforced with SiC fiber. Tsai, S.W., Springer G.S. (eds.) *Composites: Design, Manufacture and Application, Proceedings of the 8th International Conference on Composite Materials*, Honolulu, p. 19J/1–19J/10.